



Investigating the prognostic value of lateral mesorectum using preoperative high-resolution MRI in patients with rectal cancer

Siyuan Jiang¹ · Qiaoling Chen² · Shuqin Zang² · Haidi Lu² · Shiyu Ma² · Fangying Chen² · Wei Zhang¹ · Chengwei Shao² · Fu Shen²

Accepted: 22 March 2025
© The Author(s) 2025

Abstract

Background To explore the lateral mesorectum structures and develop a nomogram model for predicting the prognosis of rectal cancer (RC) patients using preoperative high-resolution magnetic resonance imaging (MRI).

Methods Patients who underwent radical resection of RC in our hospital from January 2017 to December 2018 were retrospectively analyzed. Imaging data and postoperative 3-year prognosis data of patients were collected. The lateral mesorectum was observed, and related parameters were investigated: lateral interruption of the mesorectal fascia (LI-MRF), type of the middle rectal artery (MRA), and the maximum diameter of the MRA. The impact of lateral mesorectum parameters on prognosis was determined using Cox analysis and Kaplan–Meier (KM) survival curves. A nomogram combining lateral mesorectum parameters with clinical data was constructed and its predictive performance was validated.

Results A total of 260 patients were included in this study. In preoperative high-resolution MRI, LI-MRF and MRA were observed bilaterally in all patients. Multivariate Cox regression analysis showed that the maximum diameter of the right MRA ($P=0.001$) and right LI-MRF ($P=0.016$) were predictive factors for postoperative 3-year overall survival (OS). Additionally, gender ($P=0.015$), mrT stage ($P=0.025$), and the maximum diameter of the right MRA ($P=0.002$) were predictive factors for postoperative 3-year disease-free survival (DFS). The concordance indexes (C-index) of the predictive nomogram were 0.737 for OS and 0.685 for DFS.

Conclusion Preoperative high-resolution MRI revealed that the lateral mesorectum and MRA were inherent. The right LI-MRF and the maximum diameter of the right MRA were risk factors for poor postoperative survival in RC patients.

Keywords Rectal cancer · MRI · Lateral mesorectum · Middle rectal artery

Chengwei Shao, Wei Zhang, Fu Shen have contributed equally to this work.

Siyuan Jiang, Qiaoling Chen, Shuqin Zang are the joint first authors in the paper.

✉ Wei Zhang
weizhang2000cn@163.com

✉ Chengwei Shao
cwshao@sina.com

✉ Fu Shen
ssff_53@163.com

Siyuan Jiang
jiangsiyuanjok@163.com

Qiaoling Chen
1372431158@qq.com

Shuqin Zang
zangshuqinedri@163.com

Haidi Lu
546410830@qq.com

Shiyu Ma
mashiyu_nmu@163.com

Fangying Chen
18817551679@163.com

¹ Present Address: Department of Colorectal Surgery, Changhai Hospital, The Navy Medical University, Shanghai, China

² Present Address: Department of Radiology, Changhai Hospital, The Navy Medical University, 168 Changhai Road, Shanghai 200433, China

Background

It is now academically recognized that rectal resection surgery based on the mesenteric theory has more favorable outcomes [1–6]. The goal of total mesorectal excision (TME) based on the mesenteric theory is the complete and extensive removal of the entire mesorectum [5], and its superiority in terms of outcomes has been widely demonstrated [7, 8]. However, the 5-year local recurrence rate of rectal cancer after TME is still about 10% [9]. The presence and composition of the mesorectal fascia, especially the lateral rectal structures, play an important role in surgery [10–12]. Accurate assessment of the lateral rectal structures can limit postoperative recurrence in patients with rectal cancer [13, 14].

Based on clinical surgical experience and previous research, scholars concluded that the lateral structure of the rectum inherently existed as an area of fascial fusion or dense adhesion between the mesorectal fascia (MRF), Denonvilliers' fascia, and the pelvic nerve plexus [15, 16]. When the perirectal space is separated, the lateral dense adhesion looks like a ligament on the anterolateral aspect of the mesorectum. From its anatomical structure, it is more appropriate to name the lateral structure of the rectum the lateral mesorectum. The rationale and anatomical basis for redefining the lateral rectal structures as the lateral mesorectum were demonstrated through gross and in situ histological exploration, which is the pathway of the middle rectal artery, nerves, and lymph [17–20]. However, due to the rarity of gross specimens, prognostic studies with large samples could not be conducted.

On preoperative rectal high-resolution magnetic resonance imaging (MRI), we observed the "lateral mesorectum" as an interruption of the mesorectal fascia (LI-MRF), through which the middle rectal artery (MRA) passes. This observation is consistent with in situ tissue sections and anatomical findings from gross specimens. This finding indicates that we can further confirm the existence of the lateral mesorectum by interpreting and analyzing rectal MR images of clinical patients to assess its clinical value. However, the parameters of the lateral mesorectum measured by rectal MRI for prognostic research have not been reported.

The aim of this study was to investigate the prognostic value of the lateral mesorectum and related parameters based on preoperative high-resolution MRI in RC. We aimed to build a predictive model combining this imaging approach with clinical data to provide substantial evidence supporting the theory of the lateral mesorectum and to fill the research gap regarding its impact on prognosis.

Methods

Participants

The data of patients who underwent presurgical rectal MRI in our hospital from January 2017 to December 2018 were retrospectively analyzed. The study was approved by the Ethics Committee of Changhai Hospital. Before starting the study, all patients signed written informed consent.

Inclusion criteria

- (1) Patients with rectal adenocarcinoma confirmed by pathology;
- (2) Single lesion for each patient;
- (3) Patients undergoing radical resection of RC;
- (4) Rectal high-resolution MRI performed within 2 weeks prior to surgical resection, with MR images stored in our hospital's Picture Archiving and Communication System;
- (5) Primary RC without simultaneous distant metastases and follow-up for at least three years.

Exclusion criteria

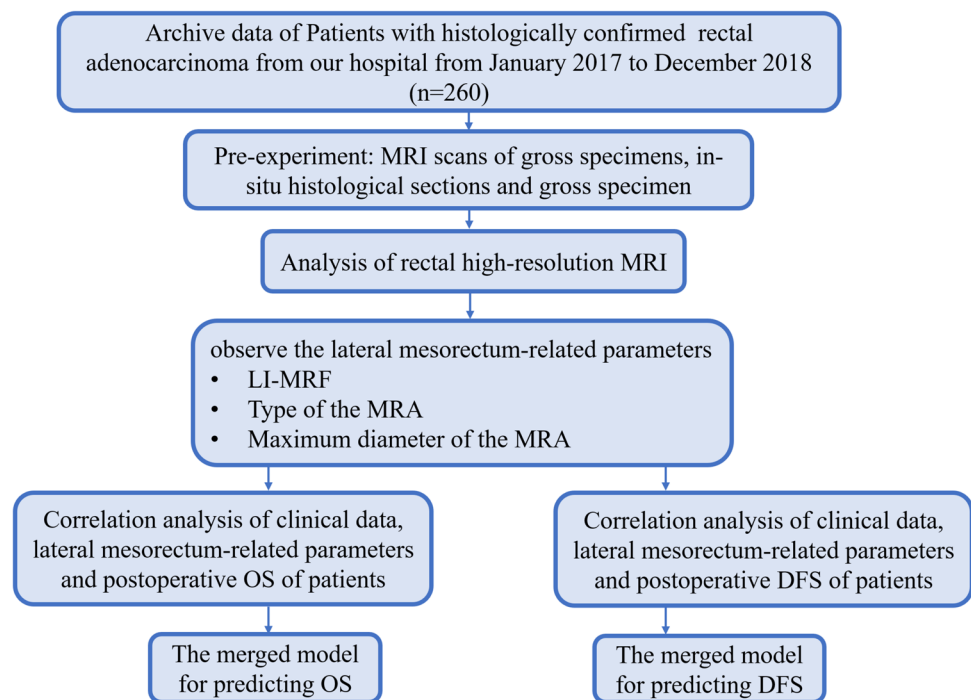
- (1) Rectal MRI showed that the lower margin of the tumor was located above the peritoneal reflection;
- (2) Receiving any local or systemic treatment prior to surgical resection (such as neoadjuvant treatment or transanal resection);
- (3) History of previous malignant tumor or pelvic surgery;
- (4) Patients with synchronous or metachronous multiple primary colorectal cancers (CRC);
- (5) Patients with any type of inherited CRC syndrome, such as Lynch syndrome or familial adenomatous polyposis (FAP);
- (6) Incomplete image sets, intracavity titanium clip artifact, or incomplete postoperative pathological report.

Baseline data were retrospectively documented from clinical and pathological databases, including age, gender, body mass index (BMI), tumor height (distance between the lower edge of the tumor and the anal verge on MRI), mrT-stage, mrN-stage, carcinoembryonic antigen (CEA), and carbohydrate antigen 19–9 (CA19-9), etc. The flowchart of this study is shown in Fig. 1.

Rectal MRI

Rectal MRI was routinely performed using 3.0 T MRI scanners (GE Discovery 750w, GE Signa HDxt, and Siemens

Fig. 1 The flowchart of this study



Skyra). The routine sequences, protocols, and parameters are shown in Supplemental Table S1. All patients fasted for 4 h before the examination. Each patient used one enema (20 mL glycerin) for bowel cleaning before the scan. An abdominal phased array coil was used. Rectal MRI sequences included sagittal T2WI, axial T1WI, high-resolution T2WI, DWI (b-value: 0, 1000 s/mm²), and contrast-enhanced T1WI (CE-T1WI), obtained in the sagittal, coronal, and axial planes. High-resolution T2WI was performed in an oblique-axial orientation, with the scanning plane perpendicular to the long axis of the bowel.

Analysis of rectal MRI

In the pre-experiment, our research group found through MRI scans of gross specimens, in-situ histological sections, and gross specimen anatomy that the lateral mesorectum and mesorectum were integrated. Before separation of the perirectal space, the lateral mesorectum appeared as an interruption of the mesorectal fascia (MRF) on the anterolateral aspect of the mesorectum (Fig. 2). In this study, measurements of the width of the lateral mesorectum were converted into measurements of the lateral interruption of the MRF (LI-MRF) at the interspinous plane on oblique-axial high-resolution T2WI.

In this study, the middle rectal artery (MRA) was defined when an artery was observed on an axial CE-T1WI to enter the mesorectum from the lateral aspects (if necessary, referring to rectal artery magnetic resonance angiography. Fig. S1). Kiyomatsu et al. [18] conducted a retrospective

study of the MRA and classified it into three types: (1) anterolateral type, branching from the prostatic artery, inferior vesical artery, or uterine artery; (2) lateral type, directly entering the mesorectum from the side; and (3) posterolateral type, entering the posterior rectal wall through the mesorectal fascia (Fig. 3a-c). Takahashi et al. [19] proposed in their study that 100% of the rectal lateral ligament contained the MRA. There was another type of MRA with multiple small branches, defined as the (4) small-branch type because of its small diameter and lack of a distinct main trunk (Fig. 3d). The diameter of the thickest artery was measured.

MR images were evaluated by two radiologists (QL.C. and SQ.Z.) with 8 and 10 years of experience in MR diagnosis, respectively, who were blinded to the clinical and pathological data. If their assessments were inconsistent, a third senior radiologist (F.S.) with 14 years of medical imaging experience made the final decision. The two radiologists measured the interrupted width of the MRF and the MRA diameters three times on each side of the mesorectum for each patient, using the average as the final result. The intra-class correlation coefficient (ICC) was used to evaluate the consistency of the two radiologists' measurements.

Follow-up

Patients were followed up every 3 months for the first 2 years after surgery, every 6 months for 3 to 5 years after surgery, and every year thereafter. At least one colonoscopy was required each year after surgery. Follow-up visits documented patient

Fig. 2 Magnetic resonance imaging and pathological images. (a) Ex vivo axial rectal high-resolution MRI of pelvic specimen; (b) Pelvic tissue sections stained with Sirius crimson ($\times 3$); (c) Axial plane of pelvic specimen after separating the perirectal space; (d) In vivo rectal high-resolution MRI of male patients; (e) In vivo rectal high-resolution MRI of female patients. 1: Seminal vesicle gland; 2: Rectum; Red arrow: the lateral interruption of the mesorectal fascia; Yellow line: the distance measurement

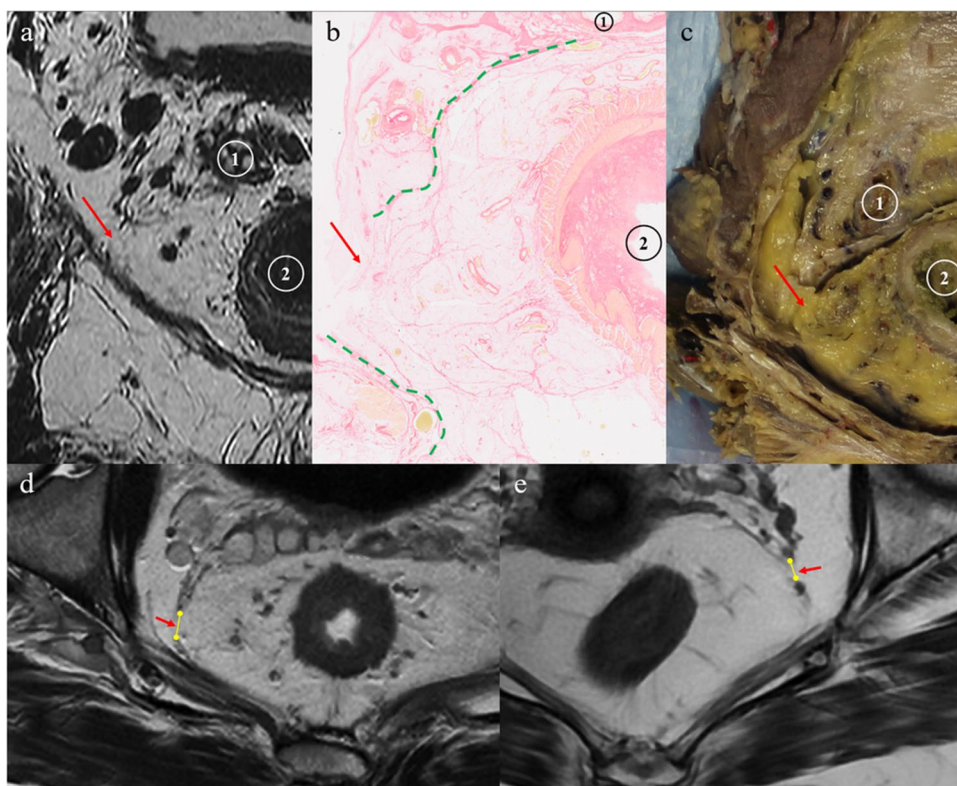
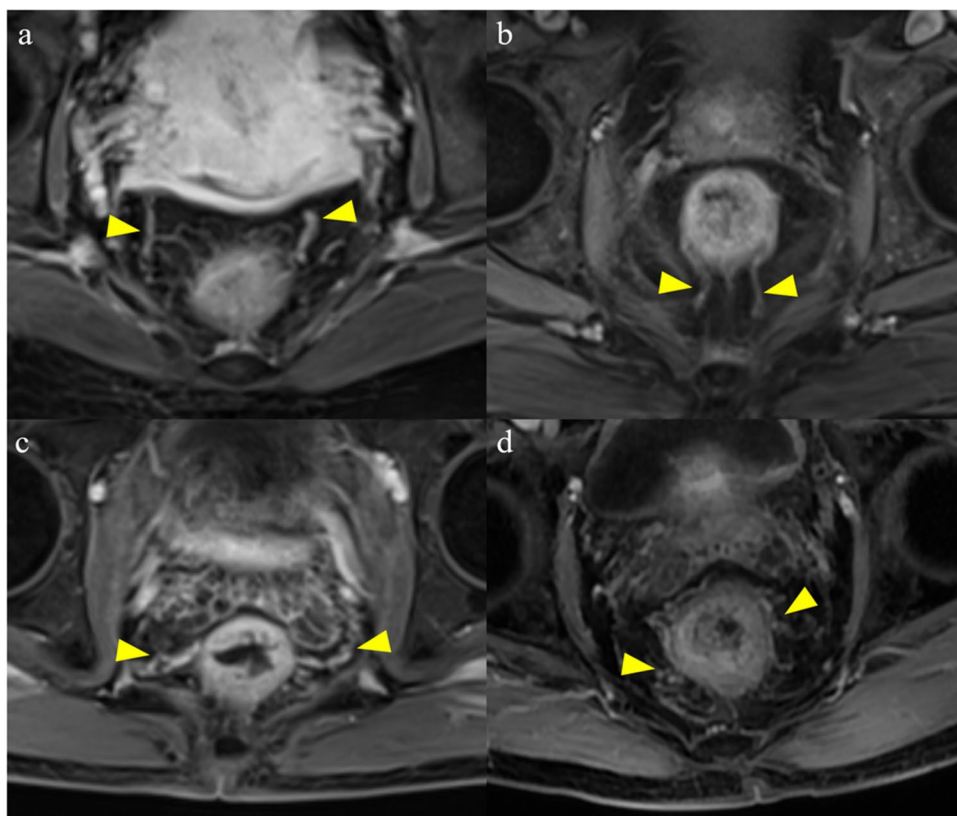


Fig. 3 Four types of the MRA. (a) antero-lateral type; (b) postero-lateral type; (c) lateral type; (d) small-branch type. Yellow arrowhead: MRA



survival, cause of death, presence of recurrence and metastasis, and location of recurrence and metastasis.

Statistical analysis

The Kolmogorov–Smirnov test was performed to assess the normality of all variables. Categorical variables are presented as frequencies and percentages. Continuous variables are presented as median with interquartile range (IQR, for non-normally distributed data) or as mean \pm standard deviation (for normally distributed data). Pearson's Chi-square test was used for categorical variables, and the t-test was used for continuous variables. The measured LI-MRF, the type of MRA, and the maximum diameter of MRA were statistically described. ICC was calculated for continuous variables (ICC = 0 to 0.49, poor agreement; 0.50 to 0.75, moderate agreement; 0.76 to 0.90, good agreement; 0.91 to 1.00, excellent agreement). Univariate and multivariate analysis of patients' overall survival (OS) and disease-free survival (DFS) were performed using Cox regression. Kaplan–Meier (KM) survival curves were plotted. The selected influencing factors were used to establish a combined model, and a nomogram was created. The receiver operating characteristic curve (ROC) of the predictive model was plotted, and a fitting curve between observed survival and predicted survival was created. Statistical analysis was performed using IBM SPSS Statistics 26.0 software. $P < 0.05$ was considered statistically significant.

Result

Patients screening

The data of patients who underwent radical surgery in our hospital from January 2017 to December 2018 were retrospectively analyzed based on inclusion and exclusion criteria. A total of 1648 patients were initially included. After excluding patients based on the following criteria: tumor located above the peritoneal reflection ($n = 740$), non-adenocarcinoma ($n = 52$), palliative surgery ($n = 37$), multiple primary RC ($n = 8$), familial adenomatous polyposis (FAP) ($n = 1$), preoperative treatment ($n = 188$), insufficient follow-up time (less than 3 years) ($n = 44$), and absence of high-resolution MRI ($n = 318$), a total of 260 patients were finally included (Table 1). The median follow-up time was 1172 days after surgery (interquartile range [IQR]: 1046–1265 days).

Statistical analysis of lateral mesorectum-related parameters

The ICC for lateral mesorectum-related parameters indicated good to excellent interobserver consistency

Table 1 Patient Characteristic

Characteristic	No. of patients (%)
Age (years)	61.6 \pm 10.2
Gender	
Male	162 (62.3)
Female	98 (37.7)
BMI (kg/m ²)	23.8 \pm 2.8
Tumor height (cm) [†]	4.4 \pm 3.0
mrT stage	
1	8 (3.1)
2	92 (35.4)
3	151 (58.1)
4	9 (3.5)
mrN stage	
0	70 (26.9)
1	115 (44.2)
2	75 (28.8)
CEA [*]	11.5 \pm 38.5
CA19-9 [*]	34.8 \pm 155.8
KRAS	
Mutant type	110 (42.3)
Wild type	150 (57.7)
NRAS	
Mutant type	99 (38.1)
Wild type	161 (61.9)
BRAF	
Mutant type	4 (1.5)
Wild type	256 (98.5)
MMR status	
pMMR	252 (96.9)
dMMR	8 (3.1)
Type of left MRA	
1	62 (23.8)
2	21 (8.1)
3	130 (50.0)
4	47 (18.1)
Type of right MRA	
1	34 (13.1)
2	19 (7.3)
3	152 (58.5)
4	55 (21.2)
Maximum diameter of left MRA (mm)	1.7 \pm 0.6
Maximum diameter of right MRA (mm)	1.6 \pm 0.4
Left lateral interruption of the MRF (mm)	12.5 \pm 4.8
Right lateral interruption of the MRF (mm)	13.5 \pm 5.3

MRF mesorectal fascia, MRA middle rectal artery

[†] The distance between the lower margin of the tumor to anal verge, measured by MRI; ^{*} Postoperative blood samples

BMI body mass index, CEA carcinoembryonic antigen, CA19-9 carbohydrate antigen 19–9

(Table S2). The correlation between lateral mesorectum-related parameters and the clinical data of the patients was analyzed, and the results are shown in Fig. S2. There was a correlation between the type of MRA, the maximal diameter of MRA, and the LI-MRF on the ipsilateral side. Comparing the left and right sides, there was a strong positive correlation between the type of MRA and the maximum diameter of MRA on both sides, but no correlation between the LI-MRF on both sides. The LI-MRF on both sides showed a strong positive correlation with the patient's BMI and no correlation with other clinical data.

The LI-MRF and MRA were observed bilaterally in all patients. Comparing the parameters related to the lateral mesorectum between the right and left sides, there were differences in the type of MRA, the maximum diameter of MRA, and the LI-MRF (*P* values of 0.000, 0.018, and 0.003, respectively). The quantitative analysis of the types of MRA revealed a moderate level of difference between the left and right sides (Cramer's *V* = 0.356). The maximum diameter of the MRA was smaller on the left side

compared to the right (1.56 ± 0.44 mm vs. 1.65 ± 0.58 mm, *P* = 0.018), and the LI-MRF was narrower on the left side (12.79 ± 4.59 mm vs. 13.56 ± 5.15 mm, *P* < 0.001). However, these differences were very small (Cohen's *d* values were 0.148 and 0.183, respectively).

Correlation analysis of lateral mesorectum-related parameters and postoperative overall survival of patients

Patients were divided into the 3-year survival group and the 3-year death group based on their 3-year OS. The baseline data of the two groups are shown in Table S3. Compared to the 3-year survival group, the 3-year death group had higher BMI (23.6 ± 2.7 vs. 25.4 ± 3.5 , *P* = 0.022), higher CA19-9 levels (22.8 ± 114.1 vs. 1164.7 ± 365.0 , *P* = 0.014), larger maximum MRA diameter on both sides (left side, *P* = 0.023; right side, *P* < 0.001), and wider LI-MRF on the right side (left side, *P* = 0.021; right side, *P* < 0.001, Fig. S3). KM

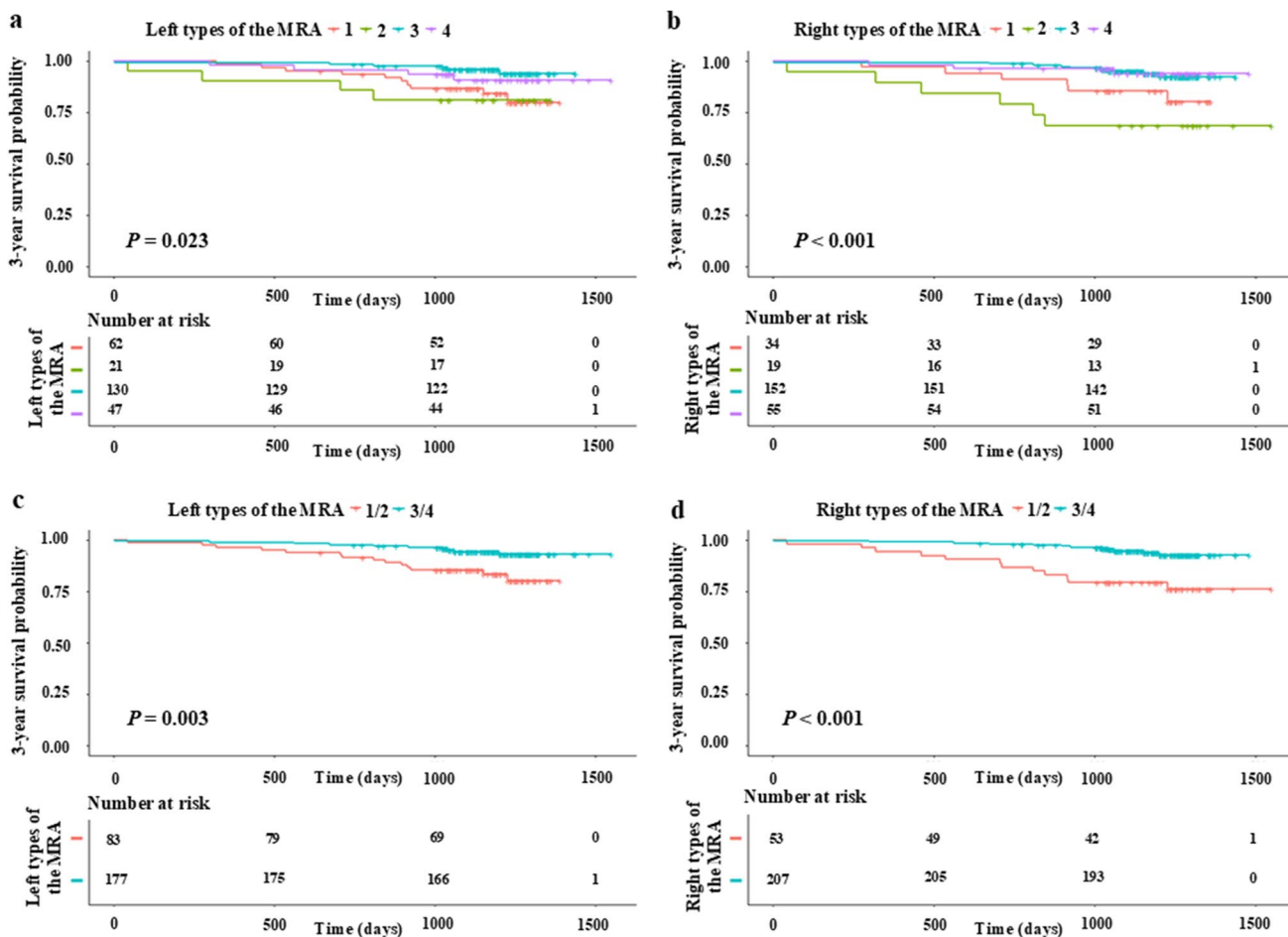


Fig. 4 KM curves of OS. (a) plotted according to the four types of left MRA; (b) plotted according to the four types of right MRA; (c) plotted according to type1/2 and type3/4 of left MRA; (d) plotted according to type1/2 and type3/4 of right MRA

curves were plotted according to the type of MRA, showing different 3-year survival rates among the four MRA types (left side $P=0.023$; right side $P<0.001$, Fig. 4a-b). Types 1 and 2 MRA were associated with poorer prognosis compared to types 3 and 4 (left side $P=0.003$; right side $P<0.001$, Fig. 4c-d).

Multivariate Cox regression showed that the maximum diameter of the right MRA ($P=0.001$, HR: 5.526, 95% CI: 2.000–15.270) and the right LI-MRF ($P=0.016$, HR: 1.100, 95% CI: 1.018–1.189) were predictors of OS (Table 2).

Correlation analysis of lateral mesorectum-related parameters and postoperative disease-free survival of patients

Patients were divided into the DFS group and non-DFS group based on whether recurrence or metastasis occurred within 3 years. The baseline data for both groups are shown in Table S4. Patients who experienced recurrence or metastasis had higher BMI (23.6 ± 2.8 vs. 25.4 ± 3.5 , $P=0.022$), higher mrT stage ($P=0.013$), a higher proportion of males ($P=0.020$), higher CA19-9 levels (18.3 ± 87.6 vs. 107.3 ± 303.8 , $P=0.024$), wider LI-MRF on the right side ($P=0.008$, Fig. S4), and larger maximum diameter of the right MRA ($P<0.001$, Fig. S4). KM curves indicated different DFS rates among the four MRA types on the right side ($P<0.001$, Fig. 5b), with types 1 and 2 MRA showing lower DFS rates compared to types 3 and 4 ($P<0.001$, Fig. 5d).

Multivariate analysis showed that gender ($P=0.015$, HR: 2.058, 95% CI: 1.152–3.678), mrT stage ($P=0.025$, HR: 2.233, 95% CI: 1.104–4.515), and the maximum diameter of the right MRA ($P=0.002$, HR: 2.706, 95% CI: 1.442–5.077) were predictive factors for DFS (Table 3).

Performance of the prognostic model

A predictive merged model was established from the selected factors, with concordance indexes (C-index) of 0.737 (95% CI: 0.624–0.849) for OS and 0.685 (95% CI: 0.611–0.758)

for DFS. The prognostic nomogram for predicting OS and DFS is illustrated in Fig. 6.

The bootstrap algorithm (500 cross-validations as a validation tool) showed satisfactory performance for the merged model, with an AUC of 0.744 (95% CI: 0.623–0.850) for 3-year OS and 0.695 (95% CI: 0.611–0.774) for 3-year DFS (Table 4, Fig. S5). The relationship between observed survival and optimism-corrected survival was evaluated through a smoothed curve fit, showing a high level of consistency between them (Fig. S6). DCA demonstrated that the merged model had a greater advantage compared to either the "all" or "none" schemes (Fig. S7).

Discussion

In this study, the lateral mesorectum and MRA were observed bilaterally in all patients on high-resolution MRI. A larger maximum diameter of the right MRA (HR: 5.526, 95% CI: 2.000–15.270) and a wider right LI-MRF (HR: 1.100, 95% CI: 1.018–1.189) were associated with shorter postoperative OS in RC patients. Additionally, a larger maximum diameter of the right MRA (HR: 2.706, 95% CI: 1.442–5.077) was linked to shorter postoperative DFS. Two predictive models were developed to forecast the prognosis of RC patients, with concordance indexes (C-index) of 0.737 for OS and 0.685 for DFS, respectively.

TME surgery, which has been developed and refined over decades, requires the complete removal of the rectum and its mesentery by sharp dissection under direct visualization. A natural, loose avascular area exists behind and in front of the rectum, serving as a surgical plane. However, this "holy plane" does not exist laterally. The debate over the lateral structure of the rectum has been long-standing [20–22]. The current mainstream research defines the lateral structure of the rectum as the lateral mesorectum, rather than the clinical term "lateral rectal ligament." The rationale and anatomical basis for redefining the lateral mesorectum involve the pathways of the MRA, nerves, and lymphatics [23–26].

Table 2 Univariate and multivariate analysis of OS

Factors	Univariate analysis			Multivariate analysis		
	HR	95% CI	P value	HR	95% CI	P value
Maximum diameter of left MRA	2.128	1.110–4.080	0.023			
Maximum diameter of right MRA	5.182	2.102–12.779	<0.001	5.526	2.000–15.270	0.001
Left LI-MRF	1.101	1.017–1.193	0.018			
Right LI-MRF	1.140	1.065–1.220	<0.001	1.100	1.018–1.189	0.016
Type of left MRA	0.314	0.139–0.706	0.005			
Type of right MRA	0.246	0.110–0.549	0.001			
BMI	1.236	1.068–1.430	0.004			
CA19-9	1.002	1.001–1.003	<0.001			

MRF mesorectal fascia, MRA middle rectal artery

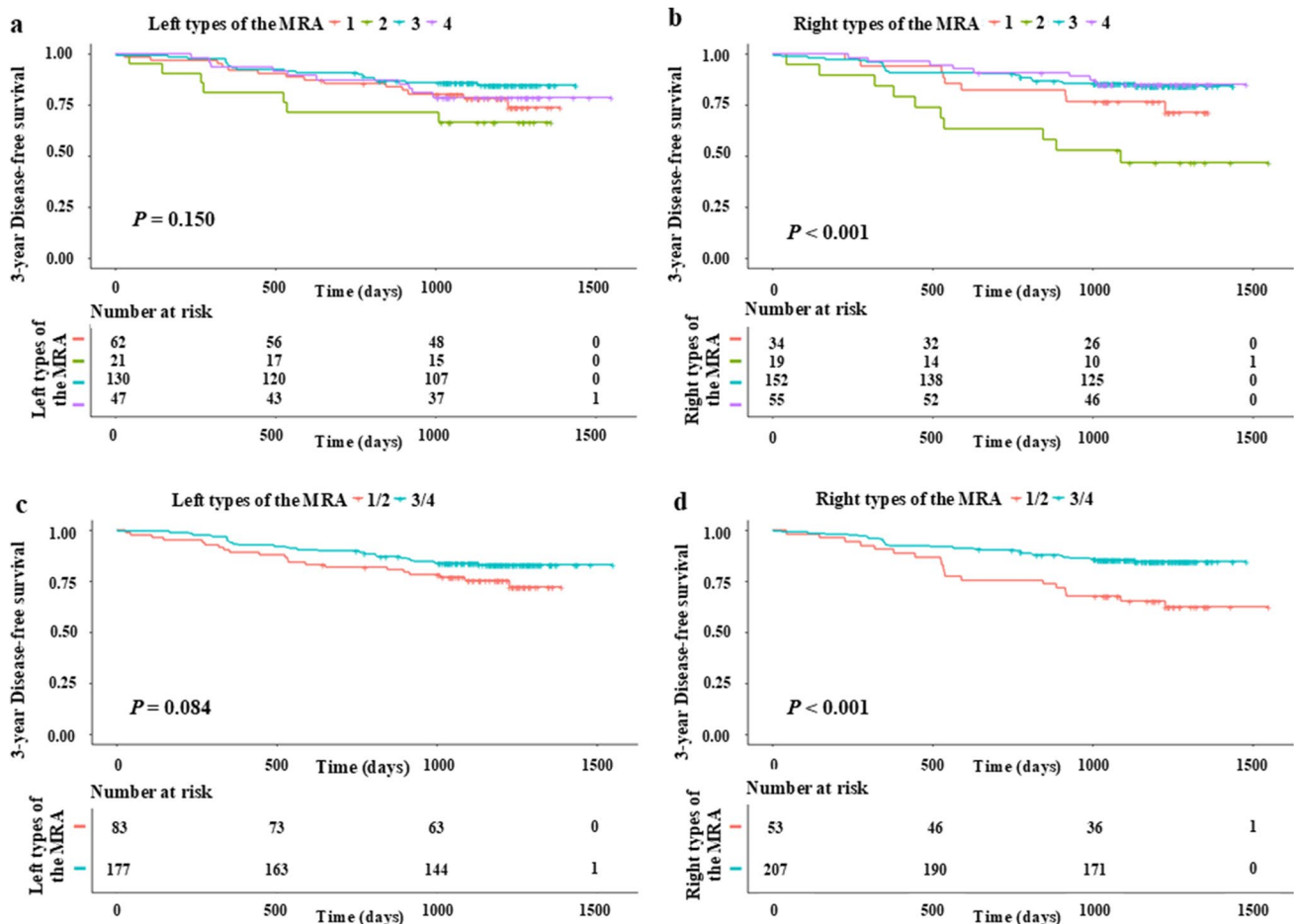


Fig. 5 KM curves of DFS. (a) plotted according to the four types of left MRA; (b) plotted according to the four types of right MRA; (c) plotted according to type1/2 and type3/4 of left MRA; (d) plotted according to type1/2 and type3/4 of right MRA

Table 3 Univariate and multivariate analysis of recurrence or metastasis

Factors	Univariate analysis			Multivariate analysis		
	HR	95% CI	P value	HR	95% CI	P value
Maximum diameter of right MRA	2.989	1.627–5.489	<0.001	2.706	1.442–5.077	0.002
Right LI-MRF	1.068	1.016–1.121	0.009			
Type of right MRA	0.386	0.218–0.683	0.001			
mrT stage	2.148	1.156–4.243	0.021	2.233	1.104–4.515	0.025
Gender	1.913	1.122–4.111	0.022	2.058	1.152–3.678	0.015
BMI	1.129	1.024–1.244	0.015			
CA19-9	1.001	1.001–1.002	0.001			

MRF mesorectal fascia, MRA middle rectal artery

In our previous studies, we demonstrated the reliability of the lateral mesorectal theory through gross specimens and in situ histological sections. By comparing high-resolution MRI, histological sections, and gross specimens of the same specimen, we found that the lateral mesorectum appears as the lateral interruption of the MRF.

The most likely reason for the impact of the lateral mesorectum on patient prognosis is lateral lymph node metastasis of RC. As early as 1951, Sauer and Bacon [27] found that metastatic lymph nodes were distributed along the "lateral ligament" in surgical specimens and proposed that the lateral ligament of the rectum played a significant role in

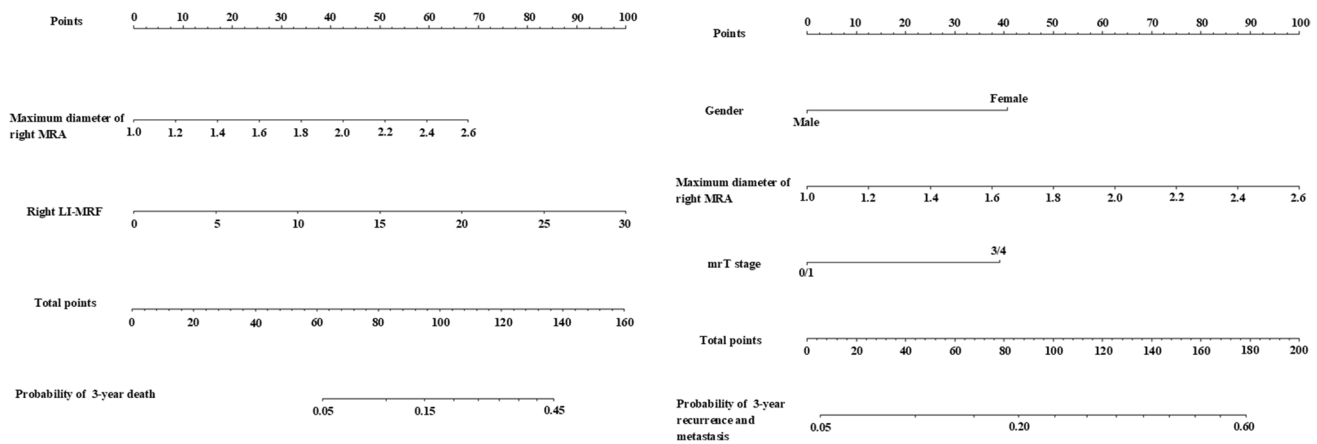


Fig. 6 Nomogram of the merged model. In the nomogram, first, a vertical line was drawn according to the value of the influencing factors label to determine the corresponding value of points. The total

points were the sum of the points above. Then, a vertical line was made according to the value of the total points to determine the probability of the 3-year survival

Table 4 The predictive performance of nomogram models

	OS model	DFS model
AUC	0.744	0.695
95% CI	0.623–0.850	0.611–0.774
Specificity	0.983	0.748
Sensitivity	0.417	0.560
Accuracy	0.931	0.712
PLR	24.583	2.219
NLR	0.593	0.588
PPV	0.714	0.346
NPV	0.943	0.877

PLR positive likelihood ratio, NLR negative likelihood ratio, NPV negative predictive value, PPV positive predictive value

lateral lymph node metastasis. In addition, our team used laparoscopic Doppler ultrasound to explore MRA during surgery and found that the lateral mesorectum contained different types of MRA regardless of the vessel diameter. Previous studies have shown that the presence and type of MRA can accurately predict lateral lymph node metastasis in rectal cancer [27–29], which is helpful for selective lateral lymph node dissection and/or chemoradiotherapy. Currently, high-resolution T2WI is recognized as a routine and mature MRI sequence for diagnosing rectal cancer [30–32]. Rectal high resolution is a scanning technique that uses thin slices, small fields of view, and increased matrix size, which further improves soft tissue resolution. High-resolution MRI can clearly show the full layer of the rectal wall, mesorectal fascia, extramural vascular invasion, lymph node metastasis, etc. Therefore, observing and analyzing the relevant parameters of the lateral mesorectum on preoperative high-resolution MRI can provide a scientific basis for clinicians to make treatment decisions. For patients with

high-risk parameters of the lateral mesorectum, neoadjuvant chemoradiotherapy and/or preventive lymph node dissection can be considered, which is our speculation.

Our results showed that the right LI-MRF and the maximum diameter of the right MRA were risk factors for poor OS in RC patients after TME surgery. The maximum diameter of the right MRA was also a risk factor for DFS. There was no correlation between lateral mesorectum-related parameters and prognosis on the left side. These results may be attributed to differences in the MRF between the left and right sides due to the rotation of the original intestine during development or the uneven distribution of lymph nodes [33, 34]. Further anatomical and embryological studies are needed to explore the specific underlying mechanisms, which are vital for improving treatment strategies and predicting outcomes.

This study had the following limitations: first, it was a single-center retrospective study, so selection bias and recall bias could not be avoided, which may affect the generalizability of the findings. Second, in our institution, the cases of RC patients treated with lateral dissections were limited. Therefore, this study did not directly analyze the relationship between the lateral mesorectum and lateral lymph node metastasis, but instead focused on postoperative survival, recurrence, and metastasis. Third, the MRA has many branches with different diameters. However, we selected the branch with the largest diameter as the representative MRA to measure its maximum diameter, which introduced inevitable subjective errors. We will strive to address these shortcomings in future research.

Conclusion

We confirmed the inherent presence of the lateral mesorectum and MRA. The LI-MRF, type of MRA, and maximum diameter of MRA can be investigated using preoperative

high-resolution MRI. Two predictive models incorporating these prognostic factors were developed to forecast the prognosis of RC patients. This study aims to assist clinicians in analyzing MRF manifestations on MRI and enhance the understanding of TME surgery.

Abbreviations MRI: Magnetic resonance imaging; MRF: Mesorectal fascia; LI-MRF: Lateral interruption of the MRF; MRA: Middle rectal artery; TME: Total mesorectal excision; RC: Rectal cancer; FAP: Familial adenomatous polyposis; BMI: Body mass index; ICC: Intra-class correlation coefficient; OS: Overall survival; DFS: Disease-free survival; KM: Kaplan-Meier

Supplementary Information The online version contains supplementary material available at <https://doi.org/10.1007/s00384-025-04871-4>.

Author contributions All authors contributed to the study conception and design. Material preparation, data collection was performed by S-Y. J, Q-L. C, S-Q. Z, Y-K. C. Data curation and analysis were performed by H-D. L, S-Y.M, F-Y.C. The first draft of the manuscript was written by S-Y.J. The manuscript was reviewed by W.Z, C-W. S, F. S. All authors commented on previous versions of the manuscript. All authors read and approved the final manuscript.

Funding This study was supported by the Guhai Project of Changhai hospital (GH145-09) and the “Yi Yuan Xin Xing” young medical talents funding project of Shanghai (project’s number: N/A).

Data availability No datasets were generated or analysed during the current study.

Declarations

Ethics approval and consent to participate This study was approved by the Ethics Committee of the the Shanghai Changhai Hospital, Naval Medical University (IRB Approval No. B2023-005).

Consent for publication Not applicable.

Competing interests The authors declare no competing interests.

Open Access This article is licensed under a Creative Commons Attribution-NonCommercial-NoDerivatives 4.0 International License, which permits any non-commercial use, sharing, distribution and reproduction in any medium or format, as long as you give appropriate credit to the original author(s) and the source, provide a link to the Creative Commons licence, and indicate if you modified the licensed material. You do not have permission under this licence to share adapted material derived from this article or parts of it. The images or other third party material in this article are included in the article’s Creative Commons licence, unless indicated otherwise in a credit line to the material. If material is not included in the article’s Creative Commons licence and your intended use is not permitted by statutory regulation or exceeds the permitted use, you will need to obtain permission directly from the copyright holder. To view a copy of this licence, visit <http://creativecommons.org/licenses/by-nc-nd/4.0/>.

References

- Coffey JC (2013) Surgical anatomy and anatomic surgery - Clinical and scientific mutualism. *Surg-J R Coll Surg E* 11(4):177–182
- Hohenberger W, Weber K, Matzel K et al (2009) Standardized surgery for colonic cancer: complete mesocolic excision and central ligation—technical notes and outcome. *Colorectal Dis* 11(4):354–64 (**discussion 364-5**)
- Heald RJ (1988) The “Holy Plane” of rectal surgery. *J Roy Soc MED* 81(9):503–508
- Heald RJ, Husband EM, Ryall RD (1982) The mesorectum in rectal cancer surgery—the clue to pelvic recurrence? *Brit J Surg* 69(10):613–616
- Liang JT, Lai HS, Huang J et al (2014) Long-term oncologic results of laparoscopic D3 lymphadenectomy with complete mesocolic excision for right-sided colon cancer with clinically positive lymph nodes. *Surg Endosc* 29(8):2394–2401
- Willaert W, Ceelen W (2015) Extent of surgery in cancer of the colon: is more better? *World J Gastroentero* 21(1):132–138
- West NP, Morris EJ, Rotimi O et al (2008) Pathology grading of colon cancer surgical resection and its association with survival: a retrospective observational study. *Lancet Oncol* 9(9):857–865
- Bertelsen CA, Neuenschwander AU, Jansen JE et al (2014) Disease-free survival after complete mesocolic excision compared with conventional colon cancer surgery: a retrospective, population-based study. *Lancet Oncol* 16(2):161–168
- Faerden AE, Naimy N, Wiik P et al (2005) Total mesorectal excision for rectal cancer: difference in outcome for low and high rectal cancer. *Dis Colon Rectum* 48(12):2224–2231
- Mori S, Baba K, Yanagi M et al (2014) Laparoscopic complete mesocolic excision with radical lymph node dissection along the surgical trunk for right colon cancer. *Surg Endosc* 29(1):34–40
- Gaudio E, Riva A, Franchitto A et al (2009) The fascial structures of the rectum and the “so-called mesorectum”: an anatomical or a terminological controversy? *Surg Radiol Anat* 32(2):189–190
- Buunen M, Lange MM, Ditzel M et al (2009) Level of arterial ligation in total mesorectal excision (TME): an anatomical study. *Int J Colorectal Dis* 24(11):1317–1320
- Tanaka A, Uehara K, Aiba T et al (2020) The role of surgery for locally recurrent and second recurrent rectal cancer with metastatic disease. *Surg Oncol* 35:328–335
- Zhang W, Zhu, XM (2020) [Reappraisal of the lateral rectal structure]. *Zhonghua Wei Chang Wai Ke Za Zhi* 23(12):1144–1148
- Corman ML (1980) Classic articles in colonic and rectal surgery. A method of performing abdominoperineal excision for carcinoma of the rectum and of the terminal portion of the pelvic colon: by W. Ernest Miles, 1869–1947. *Dis Colon Rectum* 23(3):202–5
- Fung TLD, Tsukada Y, Ito M (2020) Essential anatomy for total mesorectal excision and lateral lymph node dissection, in both trans-abdominal and trans-anal perspective. *Surg-J R Coll Surg E* 19(6):e462–e474
- Lin M, Chen W, Huang L et al (2010) The anatomy of lateral ligament of the rectum and its role in total mesorectal excision. *World J Surg* 34(3):594–598
- Kiyomatsu T, Ishihara S, Muroto K et al (2016) Anatomy of the middle rectal artery: a review of the historical literature. *Surg Today* 47(1):14–19
- Takahashi T, Ueno M, Azekura K et al (2000) Lateral ligament: its anatomy and clinical importance. *Semin Surg Oncol* 19(4):386–395
- Boyle KM, Chalmers AG, Finan PJ et al (2009) Morphology of the mesorectum in patients with primary rectal cancer. *Dis Colon Rectum* 52(6):1122–1129
- Nano M, Prunotto M, Ferronato M et al (2006) The mesorectum: hypothesis on its evolution. *Tech Coloproctol* 10(4):323–8 (**discussion 327-8**)
- Akasu T, Sugihara K, Moriya Y (2009) Male urinary and sexual functions after mesorectal excision alone or in combination with extended lateral pelvic lymph node dissection for rectal cancer. *Ann Surg Oncol* 16(10):2779–2786

23. Salerno G, Sinnatamby C, Branagan G et al (2006) Defining the rectum: surgically, radiologically and anatomically. *Colorectal Dis* 8(Suppl 3):5–9
24. Boereboom CL, Watson NF, Sivakumar R et al (2009) Biological tissue graft for pelvic floor reconstruction after cylindrical abdominoperineal excision of the rectum and anal canal. *Tech Coloproctol* 13(3):257–258
25. Marr R, Birbeck K, Garvican J et al (2005) The modern abdominoperineal excision: the next challenge after total mesorectal excision. *Ann Surg* 242(1):74–82
26. Ishii M, Shimizu A, Lefor AK et al (2018) Reappraisal of the lateral rectal ligament: an anatomical study of total mesorectal excision with autonomic nerve preservation. *Int J Colorectal Dis* 33(6):763–769
27. Sauer I, Bacon HE (1951) Influence of lateral spread of cancer of the rectum on radicability of operation and prognosis. *Am J Surg* 81(1):111–20
28. Bilhim T, Pereira JA, Tinto HR et al (2013) Middle rectal artery: myth or reality? retrospective study with CT angiography and digital subtraction angiography. *Surg Radiol Anat* 35(6):517–522
29. Iwasa Y, Koyama F, Marugami N et al (2021) The middle rectal artery detected by contrast-enhanced magnetic resonance imaging predicts lateral lymph node metastasis in lower rectal cancer. *Int J Colorectal Dis* 36(8):1677–1684
30. Chen Y, Yang X, Wen Z et al (2019) Association between high-resolution MRI-detected extramural vascular invasion and tumour microcirculation estimated by dynamic contrast-enhanced MRI in rectal cancer: preliminary results. *BMC Cancer* 19(1):498
31. Gormly K (2021) Rectal MRI: the importance of high resolution T2 technique. *Abdom Radiol* 46(9):4090–4095
32. Algebally AM, Mohey N, Szmigielski W et al (2015) The value of high-resolution MRI technique in patients with rectal carcinoma: pre-operative assessment of mesorectal fascia involvement, circumferential resection margin and local staging. *Pol J Radiol* 80:115–121
33. Savin T, Kurpios NA, Shyer AE et al (2011) On the growth and form of the gut. *Nature* 476(7358):57–62
34. Davis NM, Kurpios NA, Sun X et al (2008) The chirality of gut rotation derives from left-right asymmetric changes in the architecture of the dorsal mesentery. *Dev Cell* 15(1):134–145

Publisher's Note Springer Nature remains neutral with regard to jurisdictional claims in published maps and institutional affiliations.